Magnetic Resonance Evidence of Hypoxia in a Homozygous Alpha-Knockout of a Transgenic Mouse Model for Sickle Cell Disease

Mary E. Fabry,* Richard P. Kennan,‡ Christopher Pàszty,‖ Frank Costantini,§ Edward M. Rubin,‖ John C. Gore,‡ and Ronald L. Nagel*

**Division of Hematology, Department of Medicine, Albert Einstein College of Medicine, New York 10461; ‡Department of Diagnostic Radiology, Yale University School of Medicine, New Haven, Connecticut 06520; §Department of Genetics and Development, Columbia University, New York 10032; and ‖Human Genome Center, Lawrence Berkeley Laboratory, Berkeley, California 94720*

Abstract

All transgenic mouse models for sickle cell disease express residual levels of mouse globins which complicate the interpretation of experimental results. We now report on a mouse expressing high levels of human β^S and 100% human α-globin. These mice were created by breeding the α-knockout and the mouse β^{major}-deletion to homozygosity in mice expressing human α- and β^S-transgenes. These β^S-α-knockout mice have accelerated red cell destruction, altered hematological indices, ongoing organ damage, and pathology under ambient conditions which are comparable with those found in $\alpha^H\beta^S\beta^{S\text{-}Ant}[\beta^{MDD}]$ mice without introduction of additional mutations which convert β^S into a "super-β^S" such as the doubly mutated $\beta^{S\text{-}Antilles}$. This is of particular importance for testing strategies for gene therapy of sickle cell disease. Spin echo magnetic resonance imaging at room air and 100% oxygen demonstrated the presence of blood hypoxia (high levels of deoxygenated hemoglobin) in the liver and kidneys that was absent in control mice. We demonstrate here that transgenic mice can be useful to test new noninvasive diagnostic procedures, since the magnetic resonance imaging technique described here potentially can be applied to patients with sickle cell disease. (*J. Clin. Invest.* 1996. 98: 2450–2455.) Key words: sickle cell anemia • magnetic resonance imaging • kidney • liver • hemoglobinopathy

Introduction

Transgenic mouse models for sickle cell disease have been useful for testing hypotheses about the pathophysiology of the disease (1–7), for testing drugs which may ameliorate the course of the disease (5, 6), and for testing strategies for gene therapy of sickle cell disease (8). Several laboratories have generated transgenic mice which express high levels of human α-globin and β^S or related mutant hemoglobins (1, 2, 9–12). Mice expressing "super-β^S" have been particularly informative about the effect of the sicklable red cell on the pathophysiology of the mouse and mouse red cells (5–7, 11–13). All of these mice express residual levels of mouse globins which interfere with polymer formation (14) and may preferentially combine with human globin chains (15). The presence of mouse globins is a particular complication in the interpretation of results of gene therapy protocols where an antisickling hemoglobin is introduced. Furthermore, mice expressing a super-β^S such as $\beta^{S\text{-}Antilles}$ may not accurately reflect the success or failure of antisickling strategies due to the presence of additional amino acid residues and small, but significant, conformational changes in the hemoglobin tetramer. A mouse β-globin knockout has been available for some time (16, 17) and an α-globin knockout has been reported recently by Pàszty et al. (18); both of these knockouts can survive in the homozygous state only if rescued by a transgene which is capable of expressing high levels of human hemoglobin.

We originally reported on a line of transgenic mice which have mild pathology under ambient conditions which becomes more severe when the animals are maintained under hypoxic conditions (1, 2). More severe pathology after exposure to hypoxia would be expected because hemoglobin S polymerizes when deoxygenated and renders the red cells nondeformable which leads to the vasoocclusion that is characteristic of this disease.

More recently, we have reported on a mouse expressing both β^S and $\beta^{S\text{-}Antilles}$ which has more severe pathology under ambient conditions (13). HbS-Antilles contains, in addition to the HbS mutation at β6 (Glu→Val), a second mutation in the same chain at β23 (Val→Ile) and has low oxygen affinity and low solubility under deoxy conditions (19). We have incorporated the α-knockout into our previously reported transgenic line (1, 2) and report on the pathology observed in these mice and compare it with that found in the $\beta^S\beta^{S\text{-}Antilles}$ mice.

The presence of deoxygenated hemoglobin influences the image intensity in transverse relaxation time (T2)[1] weighted

Address correspondence to Mary E. Fabry, Ph.D., Professor of Medicine, Department of Medicine/Ullmann 915, Albert Einstein College of Medicine, 1300 Morris Park Avenue, Bronx, NY 10461. Phone: 718-430-3753; FAX: 718-824-3153; E-mail: fabry@aecom.yu.edu

Received for publication 7 June 1996 and accepted in revised form 25 September 1996.

J. Clin. Invest.

0021-9738/96/12/2450/06 $2.00
Volume 98, Number 11, December 1996, 2450–2455

1. *Abbreviations used in this paper:* $\alpha^H\beta^S$, a mouse expressing human α- and β^S-globin; α^{KK}, a mouse homozygous for the mouse α-globin knockout; β^{MDD}, a mouse homozygous for the mouse β-globin deletion; β^S, human β-globin with the sickle mutation; $\beta^{S\text{-}Antilles}$, human β-globin with the Antilles mutations; AST, aspartate amino transferase; BOLD, blood oxygen level–dependent; LDH, lactate dehydrogenase; MR, magnetic resonance; MRI, magnetic resonance imaging; ROI, region of interest; T2, transverse relaxation time; TFA, trifluoroacetic acid.

magnetic resonance (MR) images because deoxygenated hemoglobin has a different magnetic susceptibility than oxygenated hemoglobin or tissue. This effect can be exploited to generate blood oxygen level–dependent (BOLD) contrast in which tissues with more deoxygenated hemoglobin have a lower signal intensity (20). We have used this technique to detect regions with high levels of deoxygenated hemoglobin that are at risk of sickling induced vasoocclusion in our β^S-α-knockout mice noninvasively.

Methods

Mice were bled from the tail using protocols approved by the Animals Studies Committee and blood samples were analyzed for reticulocytes using the Sysmex R-1000 system (Toa, Japan) or by staining with thiazole orange and evaluating by FACS® (Lysys II; Becton Dickinson Inc., Rutherford, NJ). Serum samples were analyzed using the Technicon Chem-1 system (Technicon, Tarrytown, NY).

The globin composition was determined by HPLC using a denaturing solvent that separates the globin chains and a Vydac large-pore (300 Å) C_4 column, 4.6 × 250 mm (Separations Group, Hesperia, CA) with a modified acetonitrile/H_2O/trifluoroacetic acid (TFA) gradient similar to that used by Schroeder et al. (21) for separating human chains. Two buffers were used: A (0.18% TFA in 36% acetonitrile) and B (0.18% TFA in 46% acetonitrile). Starting with 38% B, the percentage of B was increased by 0.583%/min until all of the globin-chains were eluted.

A mixture of α-chloralose and urethane (0.1 ml/25 grams of animal weight of 0.2 grams α-chloralose and 1 gram urethane in 10 ml NaCl) was used for anesthesia. Breathing gases were administered through a hood which was placed over the head of the mouse. Oxygen and nitrogen were mixed through an anesthesia machine and pO_2 was monitored with an oxygen meter. Gases were cycled though 20% O_2/80% N_2 and 100% O_2. In most cases the gases were cycled back to the initial condition to ensure that the MR signal returned to its initial state. The animal was wrapped in cotton and a heating pad was placed nearby to insure that body temperature was maintained.

Magnetic resonance imaging (MRI) scans were acquired using a 2 Tesla GE Omega Imager. A 5.5-cm birdcage coil was used to obtain images through a coronal plane which passed through the center of the kidneys. To obtain sensitivity to BOLD effects a T2-weighted spin echo imaging sequence was used. The spin echo sequence was used instead of more conventional gradient echo sequences to monitor blood oxygenation changes because the inherently short T2* of the abdominal region gave poor quality gradient echo images and because the spin echo sequence is more sensitive to oxygen changes in small vessels. We have shown previously that BOLD effects can be monitored in brain using spin echo methods (22). The imaging parameters were an 80-mm field of view with 64 × 128 resolution (which was zero filled to 128 × 128) and a slice thickness of 4 mm (giving a voxel size of 0.625 × 0.625 × 4 mm), the echo time of the sequence was 40 ms with a repetition time of 1 s and a two-step phase cycle per image. The total acquisition time per image was ~ 2 min. Eight images were acquired during each gas administration for statistical comparison. A minimum signal to noise of 70 was obtained in all cases. To check for bulk motion in these images we calculated the signal intensity center of mass for each image. In all the data sets used for analysis, the center of mass motion was less than one pixel in both the readout and phase encode directions. We also chose a coronal plane because it showed the least sensitivity to breathing artifacts. Images were acquired on four control mice, two β^S mice, two $\beta^S\beta^{S\text{-Antilles}}$ mice, and two β^S-α-knockout mice.

Postprocessing of images was performed in MATLAB (Mathworks, Natick, MA). The region of interest (ROI) analysis (see Figs. 2 and 3) was performed by recording the signal intensity of an ROI defined by the anatomic outline of the kidney. Images which had achieved a steady state after a change of gas were used to determine the percentage change of the MR signal relative to the hyperoxic state, while transition images (usually one or two per set within the first 2–4 min after changing oxygen levels) were discarded from the analysis. The length of exposure to each gas was chosen so at least five and usually six steady state images were collected.

To visualize the location of the largest signal changes induced by changing the breathing gases, we have generated parametric activation maps that are overlaid on conventional MR images (see Fig. 4). The difference between the 100% O_2 and room air images sets was compared on a pixel by pixel basis and subjected to a Student's paired *t* test. The *t* statistic was calculated for each pixel and a map was constructed such that any *t* value greater than a threshold of three was assigned a color. Red and yellow represent positive changes with respect to increased oxygen concentration (from 20 to 100% O_2), whereas dark and light blue represent negative changes (red areas are the most hypoxic). The *P* value for the threshold of $t > 3$ (yellow light blue) was < 0.0045.

Results

Mice which coexpress the human transgenes for α- and β^S-globin and are homozygous for the deletion of mouse β^{major} were bred to homozygosity for the mouse α-knockout. We call these mice either β^S-α-knockout mice or $\alpha^H\beta^S[\alpha^{KK}\beta^{MDD}]$ mice where α^H and β^S indicate the presence of human α- and β^S-globin genes, α^{KK} indicates homozygosity for the α-knockout, and β^{MDD} indicates homozygosity for the mouse β^{major} deletion. These mice express 100% of their α-globin as human α and 60±5% of their β-globin as β^S; the balance of the β-globin is mouse β^{minor}. Red cell indices for these mice and relevant controls are shown in Table I. The red cells of β^S-α-knockout mice sickle readily when deoxygenated (Fig. 1). β^S-α-knockout mice have very high reticulocyte counts during the first 30 d of life and elevated reticulocyte counts thereafter. The spleen has a greatly expanded red pulp even in relatively young animals. The serum enzymes aspartate amino transferase (AST), alkaline phosphatase (AlkPhos), and lactate dehydrogenase (LDH) are indicative of tissue damage and are elevated in the $\alpha^H\beta^S\beta^{S\text{-Ant}}[\beta^{MDD}]$ and $\alpha^H\beta^S[\alpha^{KK}\beta^{MDD}]$ mice but not in C57B1 control mice or in $\alpha^H\beta^S[\beta^{MDD}]$ mice (Table II). LDH isozyme patterns for mouse tissues and organs were established and are

Table I. Percent Human Globin Chains and Red Cell Indices for Control and Transgenic Mice

	% α^H/all	% β^S/all	Reticulocytes < 30 d	Reticulocytes > 30 d	MVC (fl)	MCH (pg)
C57B1/6J	—	—		3.9±0.4	45.4±0.9	14.5±1.0
$\alpha^H\beta^S[\beta^{MDD}]$	55.9±2.4	74.7±2.4		4.3±0.4	43.0±1.4	14.1±0.7
$\alpha^H\beta^S\beta^{S\text{-Ant}}[\beta^{MDD}]$	58.2±0.9	78.2±2.3	22	10.0±1.0	43.5±1.5	14.9±0.5
$\alpha^H\beta^S[\alpha^{KK}\beta^{MDD}]$	100	60±5	22	13.2±2.2	40.8±0.4	13.3±0.3

Table II. Serum Enzymes in Control and Transgenic Mice

	AST	AlkPhos	LDH
C57B1/6J	51±3	114±16	419±40
$\alpha^{H}\beta^{S}[\beta^{MDD}]$	62±5	92±9	420±43
$\alpha^{H}\beta^{S}\beta^{SAnt}[\beta^{MDD}]$	147±16	217±27	636±40
	$P < 0.0005$	$P < 0.02$	$P < 0.003$
$\alpha^{H}\beta^{S}[\alpha^{KK}\beta^{MDD}]$	97±13	206±41	728±87
	$P < 0.0007$	$P < 0.02$	$P < 0.002$

All P values are versus C57Bl. For C57B1, $n = 10$; for $\alpha^{H}\beta^{S}[\beta^{MDD}]$, $n = 17$, for $\alpha^{H}\beta^{S}\beta^{S-Ant}[\beta^{MDD}]$, $n = 27$, and for $\alpha^{H}\beta^{S}[\alpha^{KK}\beta^{MDD}]$, $n = 5$.

compatible with damage to red cells, muscle, spleen, or liver. A statistically significant increase of all three enzymes was observed in the $\alpha^{H}\beta^{S}\beta^{S\text{-}Ant}[\beta^{MDD}]$ and $\alpha^{H}\beta^{S}[\alpha^{KK}\beta^{MDD}]$ mice when compared with control mice (Table II).

MR images of control and transgenic mice were obtained with a spin echo sequence while the animals were breathing room air or 100% oxygen via a hood over the head. In control animals there is no significant change in image intensity in the liver or kidneys when the breathing gas is switched from room air to 100% oxygen. However, in both the $\alpha^{H}\beta^{S}\beta^{S\text{-}Ant}[\beta^{MDD}]$ and $\alpha^{H}\beta^{S}[\alpha^{KK}\beta^{MDD}]$ mice there is a statistically significant increase in signal intensity when the breathing gas was changed from room air to 100% oxygen. These changes were largest over the liver and kidneys in the $\alpha^{H}\beta^{S}\beta^{S\text{-}Ant}[\beta^{MDD}]$ and $\alpha^{H}\beta^{S}[\alpha^{KK}\beta^{MDD}]$ mice. Fig. 2 shows image intensity in arbitrary units in the liver and kidney as a function of time for $\alpha^{H}\beta^{S}[\alpha^{KK}\beta^{MDD}]$ and control mice only.

Fig. 3 shows the change in mean kidney signal intensity for an ROI which follows the anatomic outline of the kidney. The results are averaged over eight kidneys for control mice and four kidneys for each of the other strains of mice (mean percent signal change±standard error). A significantly greater increase in signal intensity occurred when the breathing gas was changed from normal oxygen (20% O_2) to hyperoxia in the $\beta^{S}\beta^{S\text{-}Antilles}$ mice ($S = 12.7\% \pm 1.8\%$, $P < 9 \times 10^{-10}$ vs. control [C57B1] mice) and β^{S}-α-knockout mouse ($S = 13.7\% \pm 3.9\%$, $P < 0.007$ vs. control mice) when compared with control mice ($S = 2.1\% \pm 3.4\%$). The β^{S} mice showed no apparent change in signal intensity between hyperoxia and ambient air. In Fig. 4 maps of statistically derived signal changes are overlaid on anatomical images for control, $\beta^{S}\beta^{S\text{-}Antilles}$ mice, and β^{S}-α-knockout mice to highlight the areas with the largest change in signal. The maps were thresholded at a t statistic > 3 in three or more contiguous pixels where yellow and red represent pixels with the largest positive signal change that correspond to hy-

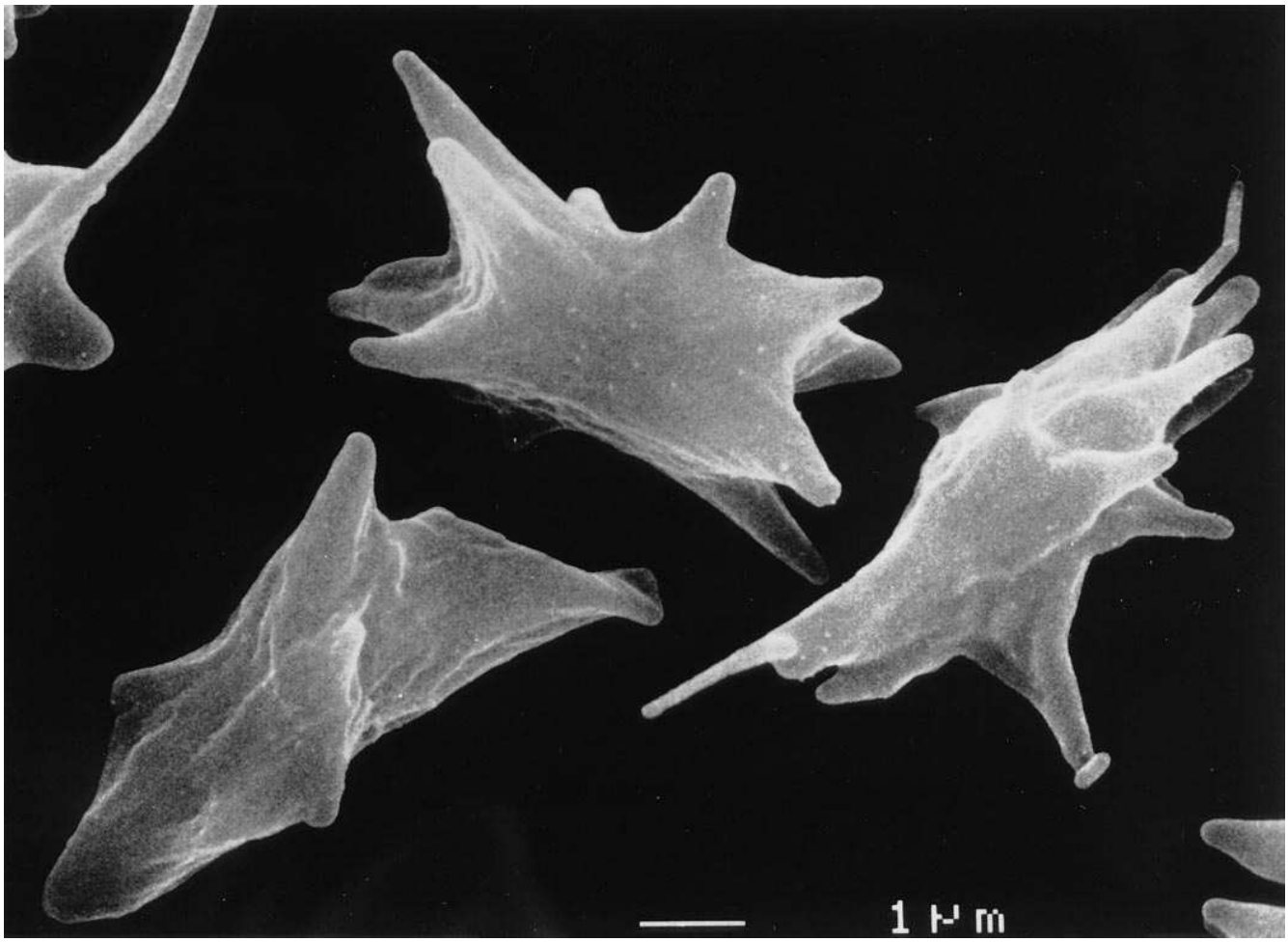

Figure 1. Scanning electron microscopy of slowly deoxygenated red cells from an $\alpha^{H}\beta^{S}[\alpha^{KK}\beta^{MDD}]$ mouse.

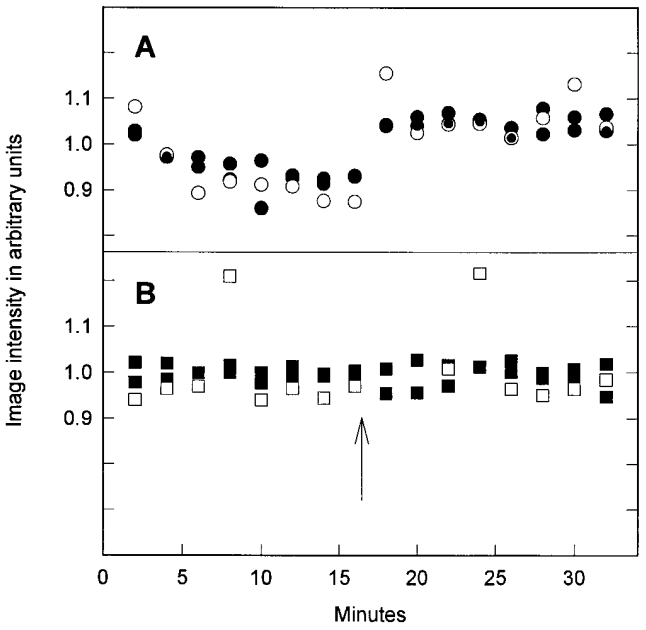

Figure 2. Time dependence of intensity changes. Signal intensity for ROIs following the anatomic outline of the kidney or an equal anatomically defined area of liver versus time for a control and a β^S-α-knockout mouse. (*A*) β^S-α-knockout mouse (●, kidney; ○, liver). (*B*) C57B1/6J control mouse (■, kidney; □, liver). Breathing gas changed to room air from 100% O_2 at zero time and then changed back to 100% O_2 at the arrow. For the β^S-α-knockout mouse, note the decrease in signal intensity after zero time and the increase in signal intensity after the arrow. The intensities were normalized by first averaging all intensities for a single organ (both room air and 100% O_2) and then normalizing to an arbitrary value of 1.0. Time points with only a single kidney value are the result of identical intensities.

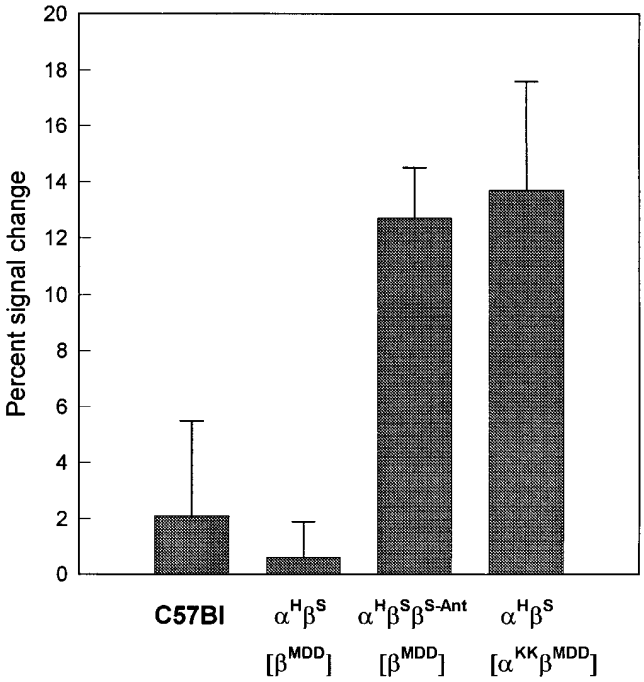

Figure 3. Relative magnitude of change for different types of mice. Percent change of average MR image intensity of an area following the anatomic outline of the kidney when breathing gas is changed from room air to 100% oxygen for four different types of mouse. Eight kidneys of four separate control (C57B1/6J) mice are averaged and four kidneys of two of each of the other three types of mouse were averaged (two mice each).

poxic regions and dark blue indicates pixels with the largest negative signal change.

Discussion

Pathophysiology of sickle mice with a homozygous α-knockout. Mice homozygous for the α-knockout ($\alpha^H\beta^S[\alpha^{KK}\beta^{MDD}]$) and expressing 60±5% β^S have significant pathology under ambient conditions, but are nevertheless capable of successful breeding and rearing pups. Young $\alpha^H\beta^S[\alpha^{KK}\beta^{MDD}]$ mice have reticulocyte counts in excess of 20% which is similar to the reticulocyte counts found in young $\alpha^H\beta^S\beta^{S\text{-}Ant}[\beta^{MDD}]$ mice. The spleen of $\alpha^H\beta^S[\alpha^{KK}\beta^{MDD}]$ mice has a greatly expanded red pulp and taken together with the increased reticulocyte count suggests enhanced red cell destruction which is a characteristic of sickle cell disease. The elevated reticulocyte count found in adult mice indicates that this process continues in adult animals, but is less severe. Red cell volume and hemoglobin content are slightly reduced in these animals (Table I). Serum enzymes are indicative of tissue and organ damage and are significantly elevated in $\alpha^H\beta^S[\alpha^{KK}\beta^{MDD}]$ mice over control mice as they are in the more extensively studied $\alpha^H\beta^S\beta^{S\text{-}Ant}[\beta^{MDD}]$ mice (Table II). AST is associated with liver damage which is well documented in $\alpha^H\beta^S\beta^{S\text{-}Ant}[\beta^{MDD}]$ mice and is elevated in both the $\alpha^H\beta^S\beta^{S\text{-}Ant}[\beta^{MDD}]$ and $\alpha^H\beta^S[\alpha^{KK}\beta^{MDD}]$ mice. Both AlkPhos and LDH are elevated in patients with sickle cell disease and are elevated in both the $\alpha^H\beta^S\beta^{S\text{-}Ant}[\beta^{MDD}]$ and $\alpha^H\beta^S[\alpha^{KK}\beta^{MDD}]$ mice. The isozyme pattern found for LDH is compatible with destruction of red cells, muscle, spleen, or liver which correlates with the known pathology of the $\alpha^H\beta^S\beta^{S\text{-}Ant}[\beta^{MDD}]$ mice.

MR results for α-knockout mice and mice with both β^S and $\beta^{S\text{-}Antilles}$. These experiments were designed to detect regions of blood hypoxia (high levels of deoxygenated hemoglobin) which may occur under ambient conditions in transgenic mice expressing sickle hemoglobin. The image intensity in spin echo images is influenced by the presence of deoxygenated hemoglobin because deoxygenated hemoglobin has a different magnetic susceptibility than oxygenated hemoglobin or tissue. The difference in magnetic susceptibility between red cells and plasma, and intravascular and extravascular spaces, results in more rapid loss of water proton transverse magnetization and ultimately results in reduced image intensity in spin echo or gradient echo pulse sequences (20). Spin echo was chosen for these experiments because of its greater specificity for changes in oxygenation in small vessels (23). Because tissue subjected to chronic hypoxia may undergo changes in water content which will affect MR image intensity, absolute image intensity is not a sensitive or reliable indicator of tissue oxygenation. However, the change in image intensity which occurs when the animal breathes air with a higher oxygen content can provide a reliable indication of regions of hypoxia.

Large (13–14%) differences in image intensity are found in the liver and kidneys of the β^S-α-knockout and the $\beta^S\beta^{S\text{-}Ant}$ mice when images obtained under room air conditions were compared with those obtained under 100% oxygen. Neither other tissues in the same animal nor the liver and kidneys of

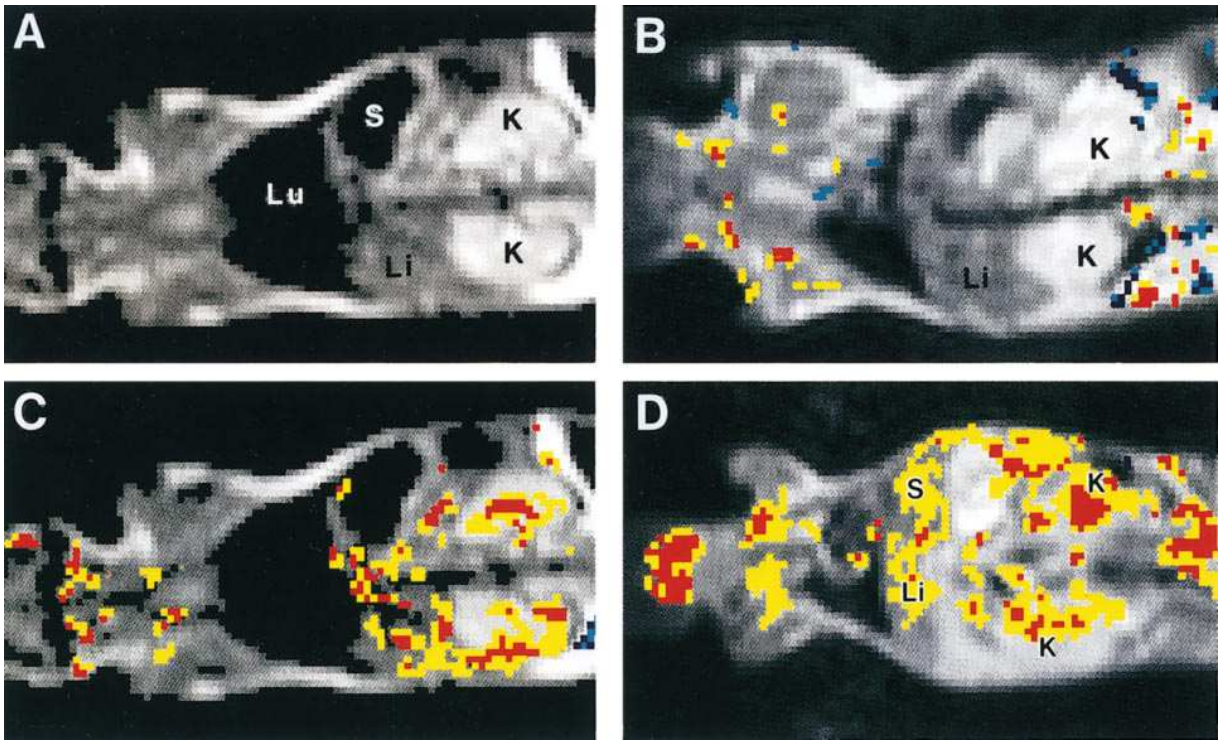

Figure 4. Areas of greatest change in intensity. MR images of mice with superimposed *t* statistic difference images (explained in Methods) obtained by comparing the room air image from the image collected while the animal was breathing 100% oxygen (*B*, *C*, and *D*). The *t* statistic was > 3 in all cases. Red and yellow areas indicate positive differences (hypoxic areas) with red indicating the largest change; light and dark blue areas indicate negative differences; gray scale areas had no statistically significant difference. Images collected at 2 T, TR, 1000 ms, TE 40 ms. (*A*) Anatomic image of the $\alpha^{H}\beta^{S}\beta^{S\text{-}Ant}[\beta^{MDD}]$ mouse in room air. *K*, kidney; *Li*, liver; *Lu*, lung; *S*, spleen. (*B*) Control mouse. Note that there are no areas with a *t* statistic > 3 over the kidneys or liver. (*C*) The same $\alpha^{H}\beta^{S}\beta^{S\text{-}Ant}[\beta^{MDD}]$ mouse seen in *A*. Note that the largest changes are over the liver and the medulla of the upper kidney. (*D*) An $\alpha^{H}\beta^{S}[\alpha^{KK}\beta^{MDD}]$ mouse. Note that the largest changes are over the medulla of the kidney. In this mouse, the spleen also shows changes characteristic of hypoxia. This may be because in this relatively young mouse there is less iron accumulation and a greatly expanded red pulp.

control or $\alpha^{H}\beta^{S}[\beta^{MDD}]$ mice exhibited differences of this magnitude. Liver and kidney are both highly vascular tissues with high metabolic rates which are susceptible to stress-induced hypoxia in normal individuals and are subject to vasoocclusion in sickle cell disease. These tissues have been shown to exhibit pathology attributable to ischemia in $\alpha^{H}\beta^{S}\beta^{S\text{-}Ant}[\beta^{MDD}]$ transgenic mice (13). Our observations are compatible with the presence of reduced hemoglobin oxygen saturation in the liver and kidneys of $\alpha^{H}\beta^{S}\beta^{S\text{-}Ant}[\beta^{MDD}]$ and $\alpha^{H}\beta^{S}[\alpha^{KK}\beta^{MDD}]$ mice. Since low hemoglobin oxygen saturation favors polymer formation, these tissues are at risk of vasoocclusion and the known pathology of the $\alpha^{H}\beta^{S}\beta^{S\text{-}Ant}[\beta^{MDD}]$ mouse which involves ischemic lesions of both the liver and kidney confirms this prediction. The observation of increased image intensity under oxygenated conditions indicates that perfusion was possible under the 100% oxygen regime, since, in the absence of perfusion, a change in blood oxygen saturation and hence image intensity would not occur. It is of interest to note that, in the kidneys of $\alpha^{H}\beta^{S}\beta^{S\text{-}Ant}[\beta^{MDD}]$ and $\alpha^{H}\beta^{S}[\alpha^{KK}\beta^{MDD}]$ mice, the medulla was the region with the largest change in intensity. The medulla is generally regarded as the most hypoxic region of the kidney (24, 25) and this is consistent with our interpretation that we are measuring in vivo hypoxia.

In a separate series of experiments, we have demonstrated that red blood cell velocity in the exposed cremaster muscle of the $\alpha^{H}\beta^{S}\beta^{S\text{-}Ant}[\beta^{MDD}]$ mouse is reduced when compared with that of control mice and increases instead of decreasing when these mice are exposed to 100% oxygen in the suffusate (7). The interpretation of this observation is that under ambient conditions there is intracellular HbS polymer formation in the red cells of $\alpha^{H}\beta^{S}\beta^{S\text{-}Ant}[\beta^{MDD}]$ mice and that exposure to elevated oxygen tension results in the polymer "melting" which then reduces blood viscosity and allows increased flow. These results are consistent with those described above.

In summary, $\alpha^{H}\beta^{S}[\alpha^{KK}\beta^{MDD}]$ mice have hematological indices and pathology comparable to that found in $\alpha^{H}\beta^{S}\beta^{S\text{-}Ant}[\beta^{MDD}]$ mice. This is significant because it allows testing strategies for gene therapy of sickle cell disease in an animal with severe pathology without introduction of additional mutations which convert β^{S} into a super-β^{S} such as the doubly mutated $\beta^{S\text{-}Antilles}$. In addition, we have demonstrated the detection of in vivo blood hypoxia in sickle transgenic mice by MRI. In patients with sickle cell disease a similar imaging protocol may allow the detection of areas at risk for sickle cell vasoocclusion.

Acknowledgments

We would like to acknowledge the technical assistance of Sandra M. Suzuka. We would also like to thank Dr. Edward Burns for his assis-

tance in obtaining the Chem1 analyses, Dr. Stephen Factor for examining the pathology specimens, and Frank Macaluso for assistance with electron microscopy.

This study was supported in part by National Heart, Lung and Blood Institute grants HL-38655 and HL-54866, and an American Heart Association (New York Affiliate) grant-in-aid.

References

1. Fabry, M.E., F. Costantini, A. Pachnis, S.M. Suzuka, N. Bank, H.S. Aynedjian, S.M. Factor, and R.L. Nagel. 1992. High expression of human β^S- and α-globins in transgenic mice: erythrocyte abnormalities, organ damage, and the effect of hypoxia. *Proc. Natl. Acad. Sci. USA.* 89:12155–12159.

2. Fabry, M.E., R.L. Nagel, A. Pachnis, S.M. Suzuka, and F. Costantini. 1992. High expression of human β^S and α-globins in transgenic mice: hemoglobin composition and hematological consequences. *Proc. Natl. Acad. Sci. USA.* 89:12150–12154.

3. Lutty, G.A., D.S. McLeod, A. Pachnis, F. Costantini, M.E. Fabry, and R.L. Nagel. 1994. Retinal and choroidal neovascularization in a transgenic mouse model of sickle cell disease. *Am. J. Pathol.* 145:490–497.

4. Bank, N., H. Aynedjian, J. Qui, M.E. Fabry, and R.L. Nagel. 1996. Renal nitric oxide synthases in transgenic sickle cell mice. *Kidney Int.* 50:184–189.

5. Trudel, M., M.E. De Paepe, N. Chretien, N. Saadane, J. Jacmain, M. Sorette, T. Hoang, and Y. Beuzard. 1994. Sickle cell disease of transgenic SAD mice. *Blood.* 84:3189–3197.

6. de Franceschi, L., N. Saadane, M. Trudel, S.L. Alper, C. Brugnara, and Y. Beuzard. 1994. Treatment with oral clotrimazole blocks Ca^{2+}-activated K^+ transport and reverses erythrocyte dehydration in transgenic SAD mice. A model for therapy of sickle cell disease. *J. Clin. Invest.* 93:1670–1676.

7. Kaul, D.K., M.E. Fabry, F. Costantini, E.M. Rubin, and R.L. Nagel. 1995. In vivo demonstration of red cell–endothelial interactions, sickling and altered microvascular response to oxygen in the sickle transgenic mouse. *J. Clin. Invest.* 96:2845–2853.

8. Fabry, M.E., S.M. Suzuka, E.M. Rubin, F. Costantini, J. Gilman, and R.L. Nagel. 1995. Strategies for amelioration of sickle cell disease: use of transgenic mice for validation of anti-sickling strategies. *In* Sickle Cell Disease and Thalassemias: New Trends in Therapy. Y. Beuzard, B. Lubin, and J. Rosa, editors. John Libbey Eurotext Ltd., London. 253–262.

9. Greaves, D.R., P. Fraser, M.A. Vidal, M.J. Hedges, D. Ropers, L. Luzzatto, and F. Grosveld. 1990. A transgenic mouse model of sickle cell disorder. *Nature (Lond.).* 343:183–185.

10. Ryan, T.M., T.M. Townes, M.P. Reilly, T. Asakura, R.P. Palmiter, and R.R. Behringer. 1990. Human sickle hemoglobin in transgenic mice. *Science (Wash. DC).* 247:566–568.

11. Rubin, E.M., H.E. Witkowska, E. Spangler, P. Curtin, B.H. Lubin, N. Mohandas, and S.M. Clift. 1991. Hypoxia-induced in vivo sickling of transgenic mouse red cells. *J. Clin. Invest.* 87:639–647.

12. Trudel, M., N. Saadane, M. Garel, J. Bardakdjuan-Michau, Y. Bloquit, J. Guerquin-Kern, P. Rouyer-Fessard, D. Vidaud, A. Pachniss, P. Romeo, et al. 1991. Towards a transgenic mouse model of sickle cell disease: hemoglobin SAD. *EMBO (Eur. Mol. Biol. Organ.) J.* 10:3157–3168.

13. Fabry, M.E., A. Sengupta, S.M. Suzuka, F. Costantini, E.M. Rubin, J. Hofrichter, G.W. Christoph, E.A. Manci, D. Culberson, D.M. Factor, and R.L. Nagel. 1995. A second generation transgenic mouse model expressing both hemoglobin S (HbS) and HbS-Antilles results in increased phenotypic severity. *Blood.* 86:2419–2428.

14. Rhoda, M.D., C. Domenget, M. Vidaud, J. Bardakdjian Michau, P. Rouyer Fessard, J. Rosa, and Y. Beuzard. 1988. Mouse alpha chains inhibit polymerization of hemoglobin induced by human beta S or beta S Antilles chains. *Biochim. Biophys. Acta.* 952:208–212.

15. Fabry, M.E., A. Sengupta, F. Costantini, A. Pachnis, and R.L. Nagel. 1992. Hemoglobin tetramer distribution in red cells of transgenic mice with high expression of HbS. *Blood.* 78:297*a*. (Abstr.)

16. Yang, B., S. Kirby, J. Lewis, P.J. Detloff, N. Maeda, and O. Smithies. 1995. A mouse model for β^0-thalassemia. *Proc. Natl. Acad. Sci. USA.* 92:11608–11612.

17. Ciavatta, D.J., T.M. Ryan, S.C. Farmer, and T.M. Townes. 1995. Mouse model of human β^0 thalassemia: targeted deletion of the mouse β^{maj}- and β^{min}-globin genes in embryonic stem cells. *Proc. Natl. Acad. Sci. USA.* 92:9259–9263.

18. Pàszty, C., N. Mohandas, M.E. Stevens, J.F. Loring, S.A. Liebhaber, C.M. Brion, and E.M. Rubin. 1995. Lethal α-thalassaemia created by gene targeting in mice and its genetic rescue. *Nat. Genet.* 95:33–39.

19. Monplaisir, N., G. Merault, C. Poyart, M.D. Rhoda, C. Craescu, M. Vidaud, F. Galacteros, Y. Blouquit, and J. Rosa. 1986. Hemoglobin S Antilles: a variant with lower solubility than hemoglobin S and producing sickle cell disease in heterozygotes. *Proc. Natl. Acad. Sci. USA.* 83:9363–9367.

20. Ogawa, S., T.M. Lee, A.S. Nayak, and P. Glynn. 1990. Oxygenation-sensitive contrast in magnetic resonance image of rodent brain at high magnetic fields. *Magn. Reson. Med.* 14:68–78.

21. Schroeder, W.A., J.B. Shelton, J.R. Shelton, V. Huynh, and D.B. Teplow. 1985. High performance liquid chromatographic separation of the globin chains of non-human hemoglobins. *Hemoglobin.* 9:461–482.

22. Constable, R.T., R.P. Keenan, A. Puce, G. McCarthy, and J.C. Gore. 1994. Functional NMR imaging using fast spin echo at 1.5 T. *Magn. Reson. Med.* 31:686–690.

23. Kennan, R.P., J. Zhong, and J.C. Gore. 1994. Intravascular susceptibility contrast mechanisms in tissues. *Magn. Reson. Med.* 31:9–21.

24. Brezis, M., and S. Rosen. 1995. Hypoxia of the renal medulla: its implications for disease. *N. Engl. J. Med.* 332:647–655.

25. Brezis, M., S. Rosen, P. Silva, and F.H. Epstein. 1984. Renal ischemia: a new perspective. *Kidney Int.* 26:375–383.